Available online at www.sciencedirect.com
ScienceDirect
Trans. Nonferrous Met. Soc. China 33(2023) 951−957
Transactions of Nonferrous Metals Society of China
www.tnmsc.cn

Electrochemical noise energy generated by nickel electroplating process

Jiao LIU[1,2], Guo-xi LI[1], Ben-feng ZHU[2,3], Xiao-qing DU[4], Yu-meng YANG[3], Guo-ying WEI[3], Zhao ZHANG[2]

1. College of Chemistry and Chemical Engineering, Hunan University, Changsha 410082, China;
2. Center of Chemistry for Frontier Technologies, Department of Chemistry, Zhejiang University, Hangzhou 310027, China;
3. College of Materials and Chemistry, China Jiliang University, Hangzhou 310018, China;
4. School of Materials Science and Energy Engineering, Foshan University, Foshan 528000, China

Received 13 December 2021; accepted 28 April 2022

Abstract: The effects of current density (J_k) and bath temperature on the structure of deposition layer of nickel and electrochemical noise energy (E^D) are studied, and the relationship between the structure of the deposit and E^D is also discussed in detail using electrochemical noise technique in coupled with the scanning electron microscopy and the glancing angle X-ray diffraction techniques. The results show that E^D theoretically mainly reflects the severity or rate of the local cathodic reaction rather than the integral cathodic reaction, and is markedly influenced by the electroplating current density (J_k)-depended nucleation/growth kinetics of the nickel deposit film. The proceeding of the nucleation (or the formation of new phase)/growth process of crystal nucleus on a foreign substrate possesses much more effect on E^D value than the subsequent homogenous growth of the already formed film particles, and the factors which can accelerate the drastic change of the electrode surface state should result in large E^D value.
Key words: nickel; electroplating; electrochemical noise energy; deposit structure

1 Introduction

Nowadays, electrochemical noise (EN) measurement has been widely used to investigate the material corrosion [1,2] and its protection [3,4], battery discharge [5,6] and plating processes [7,8], etc. Three main methods have been widely adopted to analyze the EN data, namely the statistical [9,10] (standard deviation, root mean square, skewness, kurtosis, etc.), the spectral [11,12] (fast Fourier transformer, fast wavelet technique, maximum entropy method, Hilbert−Huang transformer, etc.) and the Chaos theory-based methods [10,13]. The relative energy distribution plot (EDP), which is obtained from the fast wavelet transform (FWT) of EN data, has been regarded as the "fingerprints" of EN signals and has also been extensively applied to monitoring the metal corrosion and electroplating progress in a large number of references [14−16]. However, there is little attention on the information provided by EN energy itself.

In our earlier study [17], we explored the correlation of the EN energy with the progress of copper corrosion in different benzotriazole containing NaCl solutions. It is found that the corrosion active energy (C_{AE}), which is the sum of the energy deposited in d1−d6 crystals extracted from FWT analysis of EN, shows the opposite variation trend with the energy gap E_g derived from cyclic voltammetry. In other words, C_{AE} may be used to characterize the inhibitive performance of benzotriazole on copper corrosion. Furthermore, under certain specific or given electroplating

Corresponding author: Guo-xi LI, Tel: +86-13975146796, E-mail: liguoxi@hnu.edu.cn;
Zhao ZHANG, Tel: +86-13305816563, E-mail: eaglezzy@zju.edu.cn
DOI: 10.1016/S1003-6326(23)66158-8
1003-6326/© 2023 The Nonferrous Metals Society of China. Published by Elsevier Ltd & Science Press

conditions, the total EN energy of all d-crystals, E^D, changes oppositely with the deposit surface energy, and can be used as a measurement to evaluate the preferential orientation of deposits [18]. Besides, BEHGAM et al [19] and HADDADI et al [20] used E^D to study the corrosion process of epoxy-coated mild steel plates in 3.5 wt.% NaCl solutions and found that the sample with higher E^D exhibited much more serious corrosion. The above studies undoubtedly indicate that E^D may be a useful parameter to evaluate the electrochemical reaction process. However, to date it is still a cognitively ambiguous parameter in most situations. It is well known that metal corrosion process involves in different types (such as general, pitting and other localized corrosion) and the formation process of pitting also consists of its initial nucleation and subsequent growth. But it is not clear that the information provided by E^D mainly reflects which process. Therefore, the aim of this study is to further probe into the EN energy.

2 Experimental

The rod cathodes (6.00 mm in diameter and 10 mm in length) were made of copper with high purity (Alfa, 99.9%), and mounted in epoxy with only one cross-section exposed as the working surface. Before each experiment, the working surface was polished to mirror using abrasive papers through 500−1200 grit and 2.5 μm diamond paste, rinsed with acetone and ultrapure water, and then dried under N_2 flow. A saturated silver chloride electrode Ag/AgCl/KCl_{sat} connected through a salt bridge (KCl) was used as the reference electrode, and a large platinum foil as the counter electrode. All potentials were referred to Ag/AgCl reference electrode unless otherwise stated. To ensure that all the experiments were performed in an oxygen-free electrolyte, a conventional glass electrolysis cell with inlet and outlet was used as the electrolytic tank. The electroplating electrolyte (pH≈3.0) consisting of 100 g/L $NiSO_4·6H_2O$, 30 g/L $NiCl_2·6H_2O$ and 40 g/L HBO_3 was prepared with AR grade reagents and ultrapure water. The used galvanostatic current density of different values (0.88−4.42 mA/cm^2) was controlled by a commercial model 660A electrochemical analyzer/workstation (CH Instruments Inc., USA), and the electrodeposition was conducted in a quiescent solution for 1537 s at three different temperatures (313.15, 323.15 and 333.15 K). The electroplating noise data were acquired by a commercial PowerLab/4sp apparatus coupled with a GP Amp (ADInstruments Pty Ltd., Australia), and the sampling frequency was selected as 40 Hz. All the electroplating and measurements were tested in a faradaic cage, and performed at least three times to calculate the average value of the electrochemical noise energy. After deposition, the samples were washed with ultrapure water, dried by N_2 gas and then stored in a desiccator for further examination.

The surface morphologies were observed by a scanning transmission electron microscopy (SU−1080, Hitachi, Japan). The structure and phase composition were identified by a glancing angle X-ray diffractometer (MAXima_X XRD−7000, Shimadzu, Japan).

3 Results and discussion

3.1 Potential−time (φ−t) curve and deposit morphology

The typic φ−t curves and the corresponding deposit morphologies for nickel electroplated on Cu at 313.15 K and different depositing current densities (J_k) are shown in Figs. 1 and 2, respectively. The φ−t curves at 323.15 and 333.15 K are shown in Fig. S1 in Supporting Information (SI), and the morphologies at 323.15 and 333.15 K are shown in Figs. S2 and S3 in SI, respectively. As can be seen that, any of the φ−t curves except the lowest J_k exhibits an initially abrupt potential drop corresponding to the charging

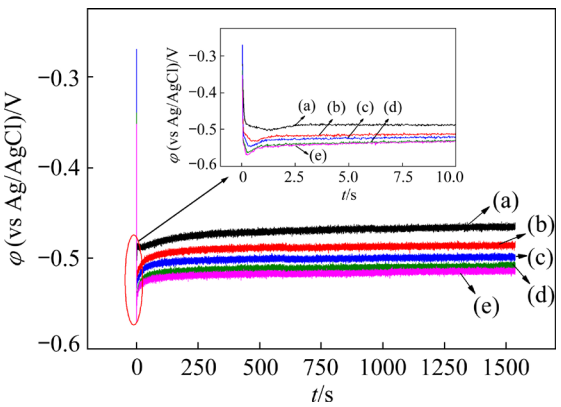

Fig. 1 Typic φ−t curves of electroplated nickel films at 313.15 K and different current densities: (a) 0.88 mA/cm^2; (b) 1.77 mA/cm^2; (c) 2.65 mA/cm^2; (d) 3.54 mA/cm^2; (e) 4.42 mA/cm^2

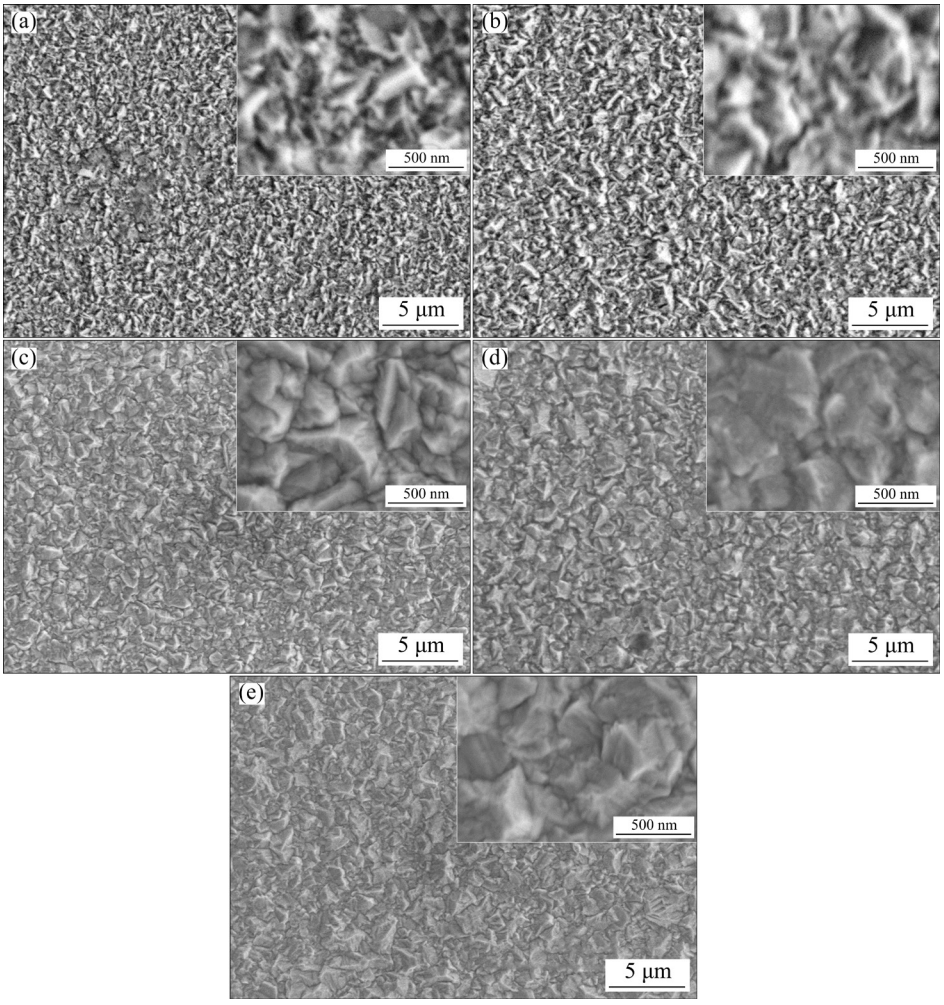

Fig. 2 SEM images of electroplated nickel films at 313.15 K and different current densities: (a) 0.88 mA/cm^2; (b) 1.77 mA/cm^2; (c) 2.65 mA/cm^2; (d) 3.54 mA/cm^2; (e) 4.42 mA/cm^2

process of the double-layer and a subsequently quick increase due to the nucleation/growth of nickel deposit (Fig. 1), which indicates that all these films may follow almost the same depositing mechanism [21]. While, much more time is requested for the $\varphi-t$ curve of the lowest J_k to reach its minimum, and also much more time is involved to gain its relative stable plateau (Inset in Fig. 1), which indicates that the deposit possesses its distinct nucleation/growth kinetics [21]. Besides, it can be observed among the deposit morphologies (Fig. 2) that the particle size increases with the increasing J_k.

3.2 Main influencing factors of electrochemical noise energy

The deposit energy (E_x) is calculated from the XRD patterns (Fig. 3 and Fig. S4 in SI) of the corresponding deposits according to the following equation [18]:

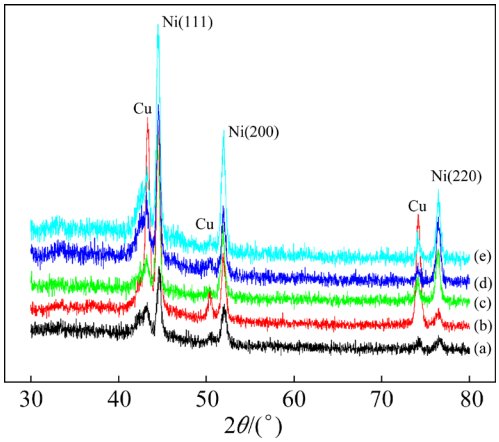

Fig. 3 XRD patterns of electroplated nickel films at 313.15 K and different current densities: (a) 0.88 mA/cm^2; (b) 1.77 mA/cm^2; (c) 2.65 mA/cm^2; (d) 3.54 mA/cm^2; (e) 4.42 mA/cm^2

$$E_x=\sum_{j=1}^{3}\left[\left(S_j\Big/\sum_{j=1}^{3}S_j\right)\cdot W_j\right] \quad (1)$$

where S_j (j=1, 2, 3) is the area of nickel (111), (200) and (220) diffraction peaks; W_j is the work function of the corresponding crystal face (j), whose values are (5.34±0.05), (5.22±0.04) and (5.04±0.02) eV for nickel (111), (200) and (220) crystal faces, respectively [22,23]. The corresponding EN energy (E^{D}) is obtained by the fast wavelet technique (FWT) analyses of EN data (Fig. 1) using the orthogonal Daubechies wavelets of the fourth order (db4),

$$E^{\mathrm{D}}=\sum_{l=1}^{J}E_l^{\mathrm{D}} \tag{2}$$

where E_l^{D} is calculated as

$$E_l^{\mathrm{D}}=\sum_{k=1}^{N/2^l}D_{l,k}^2 \quad (l=1,\ 2,\ \cdots,\ J;\ J=8) \tag{3}$$

where $D_{l,k}$ is the residual EN data (containing k data) after the l-th high-pass filtering of the original EN data..

The above analyzed results are listed in Table 1.

From Table 1, two results can be observed obviously. Firstly, E_{x} is almost independent of J_k. Secondly, the E^{D} of the lowest J_k is the largest and E^{D} keeps at a relative stable value when J_k is larger than 0.88 mA/cm^2. E_{x}, which is calculated by Eq. (1) and only depends upon the areas of diffraction peaks and their corresponding work function (W_j), mainly reflects surface energy of the deposit. According to the lowest energy principle, the nucleation and growth of new crystallites on the preformed-deposit of higher surface energy should consume smaller foreign work, and the higher the preformed-deposit surface energy, the faster the charge transfer [24]. Due to the growth and decline of different nickel crystal faces with small difference in their surface energy, especially the confine of the adopted electrode surface area, E_{x} consequently has little to do with J_k.

Nowadays, EN technique has been widely adopted to investigate the materials corrosion and protection processes. Firstly, it is well documented that the processes such as pitting or other forms of localized attack drastically change the value of anodic reaction resistance on a small area of the electrode. As a result, the information extracted from the fluctuation part (in other words, potential EN) of φ−t curves is widely used to characterize the severity of localized corrosion [25], the corrosion type [26] and even the stable/metastable pitting corrosion [27]. Similarly, such an electroplating potential EN should also mainly reflect the local (but not the entire) status of a cathode (on a small area) because the nucleation and growth of a deposit also drastically change the value of local cathodic reaction resistance. Hence, the electroplating potential EN has also been used to study the surface structure [28], the dimension [7] and the surface energy of deposit [18]. Secondly, the involved electrochemical reactions (such as the breaking of the old bonds and the formation of the new bonds) during a metal electroplating process should cause the energy transfer between the electrode system and its environment. In the process, one part of the energy is consumed as heat, and the other part (in the form of "work") expressed as the electrode potential variation results in the change of the electrode surface state (such as the formation of metal deposits). In fact, the electrode potential itself is a measurement of energy no matter in physics or in electrochemistry. The noise energy namely E^{D} is also extracted from the

Table 1 XRD parameters of nickel films electroplated at 313.15 K and different J_k and corresponding E^{D} obtained by FWT (c_{Ni}=100 g/L)

J_k/(mA·cm^{-2})	S_j			Particle size/nm					E_{x}/eV	E^{D}/V^2
	(111)	(200)	(220)	(111)	(200)	(220)	Average	$\bar{d}_{J_k}$		
0.88	3158	1858	428	17.9	14.1	15.1	15.7	16.6	5.275	0.2136
1.77	7653	2786	560	18.3	16.3	15.3	16.6	17.7	5.294	0.1484
2.65	6127	2875	2278	19.1	17.9	20.9	19.3	19.2	5.249	0.1482
3.54	6522	2398	2538	20.1	18.1	19.7	19.3	19.6	5.248	0.1377
4.42	8824	4687	2554	18.9	17.1	21.9	19.3	19	5.257	0.1387

$\bar{d}_{J_k}$ is the number-average particles size

fluctuation part of φ−t curves, especially, which is just the total energy of the potential EN (by discounting the energy contribution of DC drift using FWT technique). Consequently, E^D should also mainly reflect the severity or rate of local cathodic reaction on a small area. As elucidated above, E^D is nearly independent of J_k when J_k is larger than 0.88 mA/cm^2 mainly because the depositing processes follow almost the same nucleation/growth mechanism (Fig. 1). On the other hand, there exist distinct features of nucleation/growth behavior in φ−t curve of the lowest J_k (Fig. 1). Its dominating individuality is that much more time is requested for the electrode potential to gain the relative stable plateau, namely, much more time is involved in its initial nucleation/growth process. As the proceeding of the nucleation (or the formation of new phase)/growth process on a foreign (Cu) substrate is much more difficult than that on the same substrate (Ni deposit), and especially causes much more drastic change of the electrode surface state than the latter, the E^D of the lowest J_k is the largest (Table 1). This result may also indicate that a large or small E^D in quantitative value can be adopted to characterize the difficulty level of the initial nucleation/growth process, or even to estimate the nucleation/growth mechanism followed by different depositing processes.

Stimulated by the above findings, both the Ni films' structures electroplated at other temperatures (323.15 and 333.15 K (Figs. S2 and S3 in SI), respectively) but at different J_k, together with the corresponding potential−time data (Fig. S1 in SI) are also analyzed using XRD and FWT techniques, respectively, and the results are summarized in Table S1 in SI. As can be seen, all results undoubtedly bring about the same conclusions that E_x is nearly independent of J_k, and the E^D of the lowest J_k is the largest. Therefore, it is confirmed that E^D mainly reflects the severity or rate of local cathodic reaction on a small area, especially can provide the information about the initial nucleation/growth mechanism of a deposit.

The above findings encourage us to think about the reason why the electrode surface changes more drastically and the process possesses larger E^D value. It is considered that the faster the local charge transfer of an electrochemical process (such as electroplating, formation of inhibitor film, pitting or other localized attack) is, the more drastically the electrode surface changes, the smaller the particle size [29] or the work function [24] of the preformed deposit film possesses, the faster the charge transfer is, and the smaller the final film particle size is, the smaller the initially formed crystallites are in most cases because the nucleation is much more difficult than the growth of the already formed crystallites. Therefore, the relation- ships between J_k and E^D as well as between J_k and the product of $\bar{d}_{J_k}$ and E_x ($\bar{d}_{J_k}\cdot E_x$) are plotted (Fig. 4 and Fig. S5 in SI). Here, $\bar{d}_{J_k}$ (Table 1), which should be more suitable than the traditional arithmetic geometric mean when considering the effect of particle size on the charge transfer, is calculated according to the law of mass conservation (i.e. the mass of the total film is the sum of that with ⟨111⟩, ⟨200⟩ and ⟨220⟩ orientations) and under the hypothesis that all deposit particles are spherical, i.e.,

$$m_{total}=m_{\langle 111\rangle}+m_{\langle 200\rangle}+m_{\langle 220\rangle} \tag{4}$$

that is

$$\rho\cdot\frac{4\pi}{3}\left(\bar{d}_{J_k}/2\right)^3=\sum_{j=1}^{3}\left[\rho_j\cdot\frac{4\pi}{3}\left(d_j/2\right)^3\right] \tag{5}$$

where j is the name of Ni crystal face (j=1, 2, 3), ρ and ρ_j are the density of the total film and that with ⟨111⟩, ⟨200⟩ and ⟨220⟩ orientations, respectively. Considering $\rho\approx\rho_j$,

$$\bar{d}_{J_k}=\sqrt[3]{\sum_{k=1}^{3}\left[\left(S_j\Big/\sum_{j=1}^{3}S_j\right)\cdot d_j^3\right]} \tag{6}$$

where d_j (j=1, 2, 3) is the grain size calculated using the Scherrer formula for line broadening.

In Fig. 4, it can be clearly seen that the E^D and $\bar{d}_{J_k}\cdot E_x$ at the lowest J_k and the same temperature are the maximum and minimum, respectively. The

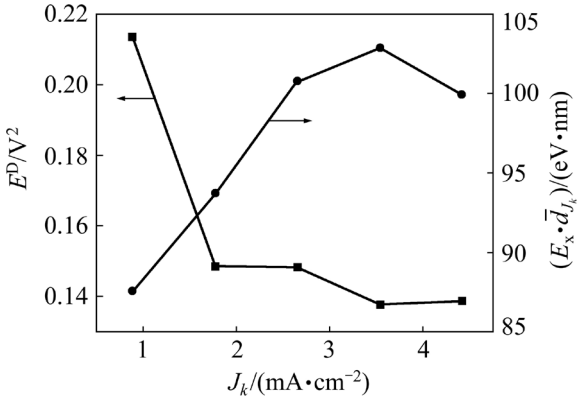

Fig. 4 Plots of E^D and $\bar{d}_{J_k}\cdot E_x$ at 313.15 K and different J_k values

former result has been attributed to that the nucleation (or the formation of new phase) process causes much more drastic change of the electrode surface than the grain growth, and there exists distinct feature of nucleation/growth mechanism in φ−t curves of the lowest J_k (Fig. 1 and Fig. S1). The latter result may indicate that the particle size (especially that of the initially formed crystallites) has a much more important effect on charge transfer than the work function, of which the reasons are as follows: (1) the $\overline{d}_{J_k}$ at the lowest J_k is the smallest (Table 1, which may be the reason why the deposition of nanomaterials is mainly performed using small J_k [30]), and (2) $\overline{d}_{J_k}\cdot E_x$ is mainly dominated by $\overline{d}_{J_k}$ because E_x has little to do with J_k as elucidated above. On the other hand, E^D keeps at a relatively stable value but with some oscillation when J_k is equal or larger than 2.65 mA/cm^2, which may indicate that other factors except $\overline{d}_{J_k}$ and E_x also influence the charge transfer of the cathode on a small area (the point discharge, the associated hydrogen evolution, etc). These factors need further investigation.

4 Conclusions

(1) The noise energy E^D mainly reflects the speed of local cathodic reaction on a small area, and is markedly changed by J_k through altering the nucleation kinetics and the growth mechanism of the deposit, i.e., E^D can provide the information about the initial nucleation/growth mechanism of a deposit.

(2) The factors that can accelerate the drastic change of the electrode surface state should bring about large E^D value. When compared with the growth of the already formed deposit particles, the nucleation (or the formation of new phase)/growth process of crystal nucleus on a foreign substrate possesses much more effect on E^D value.

(3) The particle size has a much more significant effect on charge transfer than the work function and therefore on E^D value, and E^D may also be influenced by other factors except the particle size and E_x.

Acknowledgments

This work was financially supported by the National Natural Science Foundation of China (Nos. 51771173, 52001300).

Supporting Information

Supporting Information in this paper can be found at: http://tnmsc.csu.edu.cn/download/23-p0951-2021-1492-supporting_information.pdf.

References

[1] ACOSTA G, VELEVA L, LÓPEZ J L, LÓPEZ-SAURI D A. Contrasting initial events of localized corrosion on surfaces of 2219-T42 and 6061-T6 aluminum alloys exposed in Caribbean seawater [J]. Transactions of Nonferrous Metals Society of China, 2019, 29(1): 34−42.

[2] GAI Xin, BAI Yun, LI Shu-jun, HOU Wen-tao, HAO Yu-lin, ZHANG Xing, HAN Yong, YANG Rui, MISRA R D K. In-situ monitoring of the electrochemical corrosion behavior in fluoride environment of cellular structured Ti6Al4V alloy fabricated by electron beam melting [J]. Corrosion Science, 2021, 181: 109258.

[3] YANG Guang, WANG Hai-xu, WANG Ning, SUN Rong, WONG Ching-ping. Integrated electrochemical analysis of polyvinyl pyrrolidone (PVP) as the inhibitor for copper chemical mechanical planarization (Cu-CMP) [J]. Journal of Alloys and Compounds, 2019, 770: 175−182.

[4] KANNAN P, VARGHESE A, PALANISAMY K, ABOUSALEM A S. Evaluating prolonged corrosion inhibition performance of benzyltributylammonium tetrachloroaluminate ionic liquid using electrochemical analysis and Monte Carlo simulation [J]. Journal of Molecular Liquids, 2020, 297: 111855.

[5] RUBIO M A, BETHUNE K, URQUIA A, ST-PIERRE J. Proton exchange membrane fuel cell failure mode early diagnosis with wavelet analysis of electrochemical noise [J]. International Journal of Hydrogen Energy, 2016, 41(33): 14991−15001.

[6] MAIZIA R, DIB A, THOMAS A, MARTMIANOV S. Proton exchange membrane fuel cell diagnosis by spectral characterization of the electrochemical noise [J]. Journal of Power Sources, 2017, 342: 553−561.

[7] HUANG Xian-qiu, CHEN Yu, FU Tai-wen, ZHANG Zhao, ZHAGN Jian-qing. Study of tin electroplating process using electrochemical impedance and noise techniques [J]. Journal of the Electrochemical Society, 2013, 160(11): D530−D537.

[8] RAJABALIZADEH Z, SEIFZADEH D, HABIBI-YANGJEH A. Online evaluation of electroless deposition rate by electrochemical noise method [J]. Transactions of Nonferrous Metals Society of China, 2019, 29(8): 1753−1762.

[9] ZHANG Li-jun, ZHU Xu-bei, ZHANG Zhao, ZHANG Jian-qing. Electrochemical noise characteristics in corrosion process of AZ91D magnesium alloy in neutral chloride solution [J]. Transactions of Nonferrous Metals Society of China, 2009, 19(2): 496−503.

[10] GARCIA-OCHOA E. Recurrence plots: A new methodology for electrochemical noise signal analysis [J]. Journal of Electroanalytical Chemistry, 2020, 864: 114092.

[11] JEVREMOVIC I, ERBE A. The reassigned pseudo Wigner–Ville transform in electrochemical noise analysis [J]. Physical Chemistry Chemical Physics, 2019, 21(44): 24361−24372.

[12] ROCABRUNO-VALDÉS C I, ESCOBAR-JIMÉNEZ R F, DÍAZ-BLANCO Y, GÓMEZ-AGUILAR J F, ASTORGA-ZARAGOZA C M, URUCHURTU-CHAVARÍN J. Corrosion evaluation of aluminum 6061-T6 exposed to sugarcane bioethanol−gasoline blends using the Stockwell transform [J]. Journal of Electroanalytical Chemistry, 2020, 878: 114667.
[13] CHEN An-na, CAO Fao-he, LIAO Xiao-ning, LIU Wen-juan, ZHENG Li-yun, ZHANG Jian-qing, CAO Chu-nan. Study of pitting corrosion on mild steel during wet–dry cycles by electrochemical noise analysis based on chaos theory [J]. Corrosion Science, 2013, 66: 183−195.
[14] ZHANG Tao, SHAO Ya-wei, MENG Guo-zhe, WANG Fu-hui. Electrochemical noise analysis of the corrosion of AZ91D magnesium alloy in alkaline chloride solution [J]. Electrochimica Acta, 2007, 53(2): 561−568.
[15] CUI Jun, PEI Yuang-sheng. Enhanced photocathodic protection performance of Fe_2O_3/TiO_2 heterojunction for carbon steel under simulated solar light [J]. Journal of Alloys and Compounds, 2019, 779: 183−192.
[16] COMAS C, HUET F, NGO K, FREGONESE M, IDRISSI H, NORMAND B. Corrosion propagation monitoring using electrochemical noise measurements on carbon steel in hydrogenocarbonated solution containing chloride ions [J]. Corrosion Science, 2021, 193: 109885.
[17] CHEN Yu, YANG Zhong-nian, LIU Yuan-wei, ZHANG Hong-hong, YIN Jun-ying, XIE Yan, ZHANG Zhao. In-situ monitoring the inhibition effect of benzotriazole on copper corrosion by electrochemical noise technique [J]. Journal of the Taiwan Institute of Chemical Engineers, 2017, 80: 908−914.
[18] LIU Jiao, LI Guo-xi, ZHU Ben-feng, DU Xiao-qing, YANG Yu-meng, ZHANG Zhao. Investigation of the correlation between the electrochemical noise energy and the deposit structure [J]. Journal of Electroanalytical Chemistry, 2021, 880: 114836.
[19] BEHGAM R, MAHDAVIAN M, RAMAZANI A. Fabrication of hollow carbon spheres doped with zinc cations to enhance corrosion protection of organosilane coatings [J]. Surfaces and Interfaces, 2020, 21: 100696.
[20] HADDADI S A, RAMAZANI SA A, MAHAVIAN M, ARJMAND M. Epoxy nanocomposite coatings with enhanced dual active/barrier behavior containing graphene-based carbon hollow spheres as corrosion inhibitor nanoreservoirs [J]. Corrosion Science, 2021, 185: 109428.
[21] PALOMAR-PARDAVÉ M, MIRANDA-HERNÁNDEZ M, GONZÁLEZ I, BATINA N. Detailed characterization of potentiostatic current transients with 2D−2D and 2D−3D nucleation transitions [J]. Surface Science, 1998, 399(1): 80−95.
[22] BAKER B G, JOHNSON B B, MAIRE G L C. Photoelectric work function measurements on nickel crystals and films [J]. Surface Science, 1971, 24(2): 572−586.
[23] PARK S, COLOMBO L, NISHI Y, CHO K. Ab initio study of metal gate electrode work function [J]. Applied Physics Letters, 2005, 86(7): 073118.
[24] SIEGFRIED M J, CHOI K S. Electrochemical crystallization of cuprous oxide with systematic shape evolution [J]. Advanced Materials, 2004, 16(19): 1743−1746.
[25] SHI Yan-yan, ZHANG Zhao, SU Jing-xin, CAO Fa-he, ZHANG Jian-qing. Electrochemical noise study on 2024-T3 aluminum alloy corrosion in simulated acid rain under cyclic wet–dry condition [J]. Electrochimica Acta, 2006, 51(23): 4977−4986.
[26] CAO Fa-he, ZHANG Zhao, SU Jing-xin, SHI Yan-yan, ZHANG Jian-qing. Electrochemical noise analysis of LY12-T3 in EXCO solution by discrete wavelet transform technique [J]. Electrochimica Acta, 2006, 51(7): 1359−1364.
[27] CAI Chao, ZHANG Zhao, CAO Fa-he, GAO Zuo-ning, ZHANG Jian-qing, CAO Chu-nan. Analysis of pitting corrosion behavior of pure Al in sodium chloride solution with the wavelet technique [J]. Journal of Electroanalytical Chemistry, 2005, 578(1): 143−150.
[28] ZHANG Zhao, LENG Wen-hua, CAI Q Y, CAO Fa-he, ZHANG Jian-qing. Study of the zinc electroplating process using electrochemical noise technique [J]. Journal of Electroanalytical Chemistry, 2005, 578(2): 357−367.
[29] DU L, FURUBE A, YAMAMOTO K, HARA K, KATOH R, TACHIYA M. Plasmon-induced charge separation and recombination dynamics in gold−TiO_2 nanoparticle systems: dependence on TiO_2 particle size [J]. The Journal of Physical Chemistry C, 2009, 113(16): 6454−6462.
[30] WALTER E C, PENNER R M, LIU H, NG K H, ZACH M P, FAVIER F. Sensors from electrodeposited metal nanowires [J]. Surface and Interface Analysis, 2002, 34(1): 409−412.

镀镍过程中电化学噪声能量

刘 姣[1,2]，李国希[1]，朱本峰[2,3]，杜小青[4]，杨雨萌[3]，卫国英[3]，张 昭[2]

1. 湖南大学 化学化工学院，长沙 410082；2. 浙江大学 化学系 化学前瞻技术研究中心，杭州 310027；
3. 中国计量大学 材料与化学学院，杭州 310018；4. 佛山科技大学 材料科学与能源工程学院，佛山 528000

摘 要：采用电化学噪声、扫描电子显微镜和掠射角 X 射线衍射等技术，研究电沉积电流密度(J_k)和镀液温度对 Ni 沉积层结构和电化学噪声能量(E^D)的影响规律，并详细探讨沉积层结构与 E^D 之间的关系。结果表明：E^D 主要反映电极表面状态的剧烈变化程度或局部阴极的反应速率，而不是反映整体阴极的反应速率；与 J_k 密切相关的 Ni 镀层初始成核/生长机制对 E^D 产生显著影响。晶粒在异质基底上的成核(新相的形成)/生长过程对 E^D 的影响远远大于薄膜晶粒的后续同质生长过程对 E^D 的影响，能够加速电极表面状态剧烈变化的因素都能导致 E^D 值的增加。

关键词：镍；电镀；电化学噪声能量；镀层结构

(Edited by Wei-ping CHEN)